



Synthesis and *in vitro* assessment of anticholinesterase and antioxidant properties of triazineamide derivatives

Murali Vatturu¹, Kandrakonda Yelamanda Rao², Valaparla Bala Yesu¹, Shaik Jeelan Basha², Tanguturi Prakash Guptha³, Donka Suresh Babu¹, Kethineni Sajitha¹, Gundlapalli Pavan

Kalyan¹, Amooru Gangaiah Damu^{**2}  & Doddaga Srinivasulu^{*1} 

¹Department of Chemistry, Sri Venkateswara University, Tirupati, Andhra Pradesh, 517501, India

²Bioorganic Chemistry Research Laboratory, Department of Chemistry, Yogi Vemana University, Kadapa, Andhra Pradesh, 516005, India

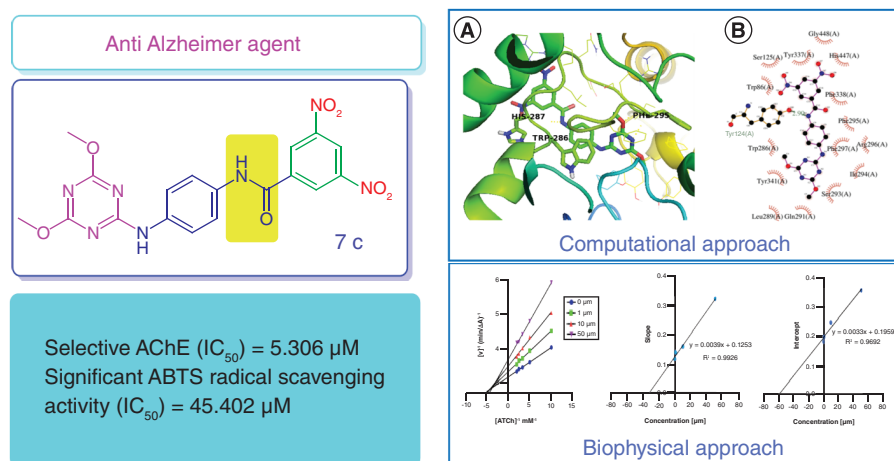
³Department of Chemistry, Indrashil University, Ahmadabad, Gujarat, 382740, India

*Author for correspondence: doddaga_s@yahoo.com

**Author for correspondence: agdamu01@gmail.com

Aim: Cholinesterase inhibitors and radical scavengers have been recognized as powerful symptomatic anti-Alzheimer's disease agents. Hence, the present study aimed to develop new triazineamides as potent anticholinesterase and antioxidant agents. **Methods:** Triazineamide (**7a–i**) derivatives were synthesized using cyanuric chloride via nucleophilic substitution followed by condensation. Ellman assay, 2,2-azino bis(3-ethylbenzthiazoline-6-sulfonic acid) radical scavenging assay and molecular docking studies with Autodock 4.2.3 program were conducted. **Results:** Triazineamide **7c** was assessed as a potent, selective and mixed-type dual inhibitor of acetylcholinesterase, with and IC_{50} of $5.306 \pm 0.002 \mu M$, by binding simultaneously with the catalytic active and peripheral anionic sites of acetylcholinesterase, and it had strong 2,2-azino bis(3-ethylbenzthiazoline-6-sulfonic acid) radical scavenging abilities. **Conclusion:** These results suggest that triazineamides may be of interest to establish a structural basis for new anti-Alzheimer's disease agents.

Graphical abstract:



First draft submitted: 15 August 2022; Accepted for publication: 21 November 2022; Published online: 20 December 2022

Keywords: ABTS radical scavenging activity • Alzheimer's disease • cholinesterase • molecular docking

A multifactorial neurodegenerative disorder, Alzheimer's disease (AD), which mostly affects elder people, is the foremost cause of dementia [1,2]. Accumulation of amyloid- β ($A\beta$) oligomers, neurofibrillary tangles and hyper-

newlands
press

phosphorylated tau proteins and the loss of synapses and neurons in the cerebral cortex and subcortical regions of the brain have been identified as the multiple, interconnected pathophysiological hallmarks of the initiation and development of AD, leading to the deterioration of memory and cognition [3–5]. This severe disease strongly affects patients and their families, friends and caregivers for years or even decades, putting intense financial and emotional pressures on them. Recent reports disclosed the existing costs of the disease per year as a trillion US dollars, and that is forecast to double by 2030 [6]. Though the etiology of AD remains far from understood, several hypotheses, such as cholinergic, amyloid, oxidative stress and metal chelation hypotheses, have been raised by scientists [7]. The cognitive impairment in AD patients is attributed to a low level of acetylcholine (ACh), as acetylcholinesterase (AChE) and butyrylcholinesterase (BChE) metabolize it to acetate and choline molecules [8]. Therefore, in the 1990s, cholinesterase inhibitors such as donepezil, galantamine, huperzine A and rivastigmine, which increase the amount of ACh by inhibiting AChE and BChE, were introduced as first-line therapeutics against AD [9,10]. Soon it became clear that these drugs only ameliorate the learning and memory functions, without preventing progressive neurodegeneration. Nonetheless, cholinesterases are still considered prominent biological targets in the design of multifunctional agents [10].

In recent years, numerous studies have shown attention to the role of free radical formation and oxidative cell damage in the pathogenesis of AD. The three main proposed mechanisms through which antioxidants may play their protective role are H atom transfer, single electron transfer and metal chelation [11]. Most of the studies have revealed that oxidative damage may encourage the emergence of amyloid fibrils, neurofibrillary tangles, neuroinflammation and mitochondrial dysfunction, which induce a vicious cycle of pathogenesis in AD [12]. Thus, the drugs aimed in clearing or avoiding the formation of the free radicals possibly useful for either the prevention or efficient treatment of AD. On the other hand, metal ions such as Cu^{+2} , Fe^{+2} , Zn^{+2} and Al^{+3} may have a major role in the pathogenesis of AD [13]. Metals have been observed to progressively accumulate in AD patients during disease progression from moderate to severe AD. The abnormal accumulation of metals is closely associated with the formation of A β plaques and neurofibrillary tangles [14]. Unusual levels of redox-active metal ions may contribute to the production of reactive oxygen species, which promote oxidative stress, thus contributing to AD pathogenesis [15]. Therefore, lowering the concentration of brain metals by chelating represents an additional rational approach for the treatment of AD.

In this context, as part of the continuing efforts to find multifunctional agents against AD, the development of triazine-based anticholinesterase congeners with antioxidant properties was planned in the present work. 1,3,5-triazine (s-triazine) is a quite stable and very fascinating chemical core found in many synthetic and natural products [16]. Since its symmetrical structure facilitates the synthesis of a diverse set of analogs, such as 2-, 4-, 6-mono, di- and tri-substituted, symmetrical and nonsymmetrical compounds bearing different substituents, it offers access to a variety of useful molecules [17,18]. Furthermore, the reactivity and sensitivity for nucleophilic substitutions of functional groups on the triazine ring appear to be different and thus assist the incorporation of three different nucleophilic fragment groups on the triazine ring [19]. Several structure–activity relationship studies revealed that the triazine scaffold acts as an anchor to make optimal binding interactions with target proteins and ring nitrogens provide enhanced activity via complexation with metals [20–23]. The heteroaromatic triazine ring is also reported to contribute to the binding affinity via π - π stacking and hydrogen-bonding interactions with the target protein receptors [21,24–29]. In addition, the triazine ring has been known to contribute to the steric properties of molecules. For example, coupling the triazine ring with aniline derivatives allow the molecules to adopt the *s-cis* conformation, which makes favorable binding interactions with the targets while relieving the steric strain of the molecules post-enzyme binding [30–32]. As a result, compounds consisting of s-triazine moiety were reported to have wide practical applications in numerous fields (in particular, medicinal chemistry) owing to their broad spectrum of pharmacological actions (e.g., antimicrobial, antifungal, antimalarial, antiamoebic, anticancer, antileishmanial, antiviral, antitubercular, carbonic anhydrase inhibitory, adenosine receptor antagonist, carbonic anhydrase inhibitory and cathepsin B inhibitory activities) and were mainly ascribed to the azomethine moiety in the s-triazine scaffold [21]. On the other hand, triazine-based analogs known to have selective binding abilities with biological targets due to the presence of both hydrogen-bond donor and acceptor sites. Thus, s-triazine cores have attracted researchers to choose this scaffold as a basic pharmacophore to develop a wide variety of medicinally important compounds [33]. Consequently, remarkable growth has been found in the literature on the evaluation of s-triazine derivatives as promising moieties as healthcare agents [34–41].

Lolak *et al.* identified bis-sulfonamide 1,3,5-triazine derivatives as potential AChE inhibitors as they fit well in the binding site of AChE and had π - π stacking and H-bonding interactions with the prominent amino acid residues in

the binding site. Further, 1,3,5-triazine-substituted ureido benzenesulfonamides were assessed as promising metal chelating and antioxidant agents, as well as selective AChE inhibitors over BChE, better than the standard drug, galantamine [42]. Later, benzenesulfonamide incorporating 1,3,5-triazine moieties were found to have moderate antioxidant potential along with excellent AChE inhibitory potential [43]. Ansari *et al.* reported that triazine-containing molecules have potential inhibition against lipopolysaccharide-induced cell death in the PC12 cell line.

Iraji *et al.* demonstrated triazine analogs as multitarget ligands for AD with potent inhibitory activities against the BACE-1 enzyme and no toxicity against PC12 neuronal cell lines [44]. 5,6-diphenyl triazine-thio methyl triazole hybrids were evaluated as multifunctional agents in AD by Yazdani *et al.* [45]. Their excellent inhibitory activity for BACE-1 was attributed to their deep penetration into the binding site of BACE-1 enzyme via H-bonding.

Gonzalez *et al.* evaluated molecules containing triazine-bridged systems with cyclen units with potential antioxidant and metal chelation activities [46]. Maqbool *et al.* identified cyanopyridine-triazine analogs as potent for cholinesterase inhibition, A β ₁₋₄₂ disaggregation, oxidative stress relief, lowered cytotoxicity and neuroprotection against A β ₁₋₄₂-induced toxicity [47]. Hence, in the present study, the authors designed the synthetic strategy of 1,3,5-triazine derivatives starting from cyanuric chloride and incorporating amide linkage for fictionalization by assuming that it amplifies the diversity in target molecules and offers further sites for binding with biological targets. Herein, they report a new series of amides encompassing a s-triazine core and 1,4-diaminobenzene with different amide moieties. Evaluation of their anticholinesterase and antioxidant activities and the binding capacities of some novel triazine derivatives with acetylcholinesterase through docking studies are also discussed.

Materials & methods

Chemistry

All the chemicals were obtained from commercial suppliers and were used directly without purification. All reactions were monitored by thin layer chromatography (TLC) and purification of compounds by column chromatography over silica gel (60–120). IR spectra were performed on a SHIMDZU-8400 spectrometer. For intermediates and target compounds, ¹H and ¹³C NMR spectra were measured on a Bruker spectrometer at 400 MHz, using CDCl₃/DMSO-d₆ solvents, and tetramethylsilane was used as an internal standard, δ parts per million and *J* in hertz. ESI-MS was determined on Xevo TQD Quadrupole (XVEO-TQD-QCA583) mass spectrometer.

Synthesis

Synthetic procedure of 2-chloro-4,6-dimethoxy-1,3,5-triazine (2)

Cyanuric chloride (**1**; 2.7 mmol, 0.50 g), NaHCO₃ (6.5 mmol, 0.55 g) and MeOH (5 ml) were placed into a round-bottom flask. The reaction mixture was stirred for 30 min at 0°C, continuing for 1.5 h to attain the room temperature; then the temperature was raised to 50°C and the mixture was refluxed for 2 h. After completion of the reaction, the solvent was concentrated under vacuum to get the crude. The crude was extracted three-times with dichloromethane (3 × 15 ml) and brine solution. The organic layer was separated and concentrated under vacuum to get the product, which was purified by column chromatography (CC) over silica gel (n-hexane/EtOAc; 10:2) to yield compound **2** (79%).

Synthetic procedure of tert-butyl (4-[(4,6-dimethoxy-1,3,5-triazin-2-yl)amino]phenyl) carbamate (4)

An intermediate **2** (1.1 eq) and Na₂CO₃ (2 eq) were dissolved in acetone then 4-(Boc-amino) aniline (1 eq) was added dropwise under stirring over a period of 30 min at 0°C. Further, the reaction mixture was stirred for 3.5 h and then poured into water. The obtained pale yellow solid was filtered to offer carbamate compound **4** (78.5%).

Synthesis of N1-(4,6-dimethoxy-1,3,5-triazin-2-yl)benzene-1,4-diamine (5)

HCl (4M) was added to a solution of compound **4** in dioxane and stirred at room temperature for 1 h. After completion, the solvent was dried and the residue was recrystallized from acetonitrile to get diamine compound **5**: white solid with a yield of 72%; melting point (mp): 235–237°C; IR(KBr) ν_{max} : 3410, 3213, 3043, 2993, 1755, 1654, 1593, 1508, 1176, 1111, 837 cm⁻¹; ¹H and ¹³C NMR: see Tables 1 & 2; ESI-MS *m/z*: 248.22 [M+H]⁺, Calcd. for C₁₁H₁₃N₅O₂.

Table 1. ¹H NMR data of 1,3,5-triazine derivatives 7a–i.

Proton	7a	7b	7c	7d	7e	7f	7g	7h	7i
7-NH	7.87 (1H, brs)	7.72 (brs, 1H)	9.15 (brs, 1H)	7.86 (brs, 1H)	8.00 (brs, 1H)	8.04 (brs, 1H, 7'-N-H)	7.82 (brs, 1H)	7.68 (brs, 1H)	8.05 (brs, 1H)
2' and 6'	7.84 (2H, d, <i>J</i> = 8.4 Hz)	7.56 (d, 2H, <i>J</i> = 8.8 Hz)	7.71 (d, 2H, <i>J</i> = 8.4 Hz)	7.65 (d, 2H, <i>J</i> = 9.4 Hz)	7.76 (d, 2H, <i>J</i> = 8.4 Hz)	7.67 (d, 2H, <i>J</i> = 9.2 Hz, 2'-H and 6'-H)	7.92 (d, 2H, <i>J</i> = 8.0 Hz)	7.66 (d, 2H, <i>J</i> = 8.0 Hz)	7.71 (d, 2H, <i>J</i> = 8.8 Hz)
3' and 5'	7.65 (m, 2H)	7.62 (d, 2H, <i>J</i> = 8.8 Hz)	7.61 (d, 2H, <i>J</i> = 8.4 Hz)	7.61 (d, 2H, <i>J</i> = 9.4 Hz)	7.65–7.63 (m, 2H)	7.63 (d, 2H, <i>J</i> = 9.2 Hz, 3'-H and 5'-H)	7.21 (d, 2H, <i>J</i> = 8.0 Hz)	7.59 (d, 2H, <i>J</i> = 8.0 Hz)	7.61 (d, 2H, <i>J</i> = 8.8 Hz)
2'' and 6''	7.60 (m, 2H)	–	9.19 (d, 2H, <i>J</i> = 2.1 Hz)	7.31 (t, 1H, <i>J</i> = 8.0 Hz)	7.39 (d, 1H, <i>J</i> = 8.4 Hz)	7.56 (d, 1H, <i>J</i> = 8.0 Hz, 6''-H),	7.90 (d, 2H, <i>J</i> = 8.0 Hz)	7.37 (m, 2H)	9.21 (m, 1H)
4''	–	7.52 (t, 1H, <i>J</i> = 4.8 Hz)	9.98 (s, 1H)	8.13 (t, 1H, <i>J</i> = 8.0 Hz)	–	7.17 (t, 1H, <i>J</i> = 7.6 Hz, 4''-H)	–	–	–
3'' and 5''	7.48 (2H, d, <i>J</i> = 8.4 Hz)	7.71 (d, 1H, <i>J</i> = 4.8 Hz) 7.09 (d, 1H, <i>J</i> = 4.8 Hz)	–	7.20–7.15 (m, 1H) 7.98–7.96 (m, 1H)	7.45 (s, 1H) 7.50 (d, 1H, <i>J</i> = 2.1 Hz)	7.94 (d, 1H, <i>J</i> = 8.0 Hz, 3''-H) 7.45 (t, 1H, <i>J</i> = 7.6 Hz, 5''-H)	7.18 (d, 2H, <i>J</i> = 8.0 Hz)	7.02 (d, 2H, <i>J</i> = 8.0 Hz)	9.19 (m, 2H)
7'', 8'' and 9''	–	–	–	–	–	–	–	–	7.97 (m, 3H)
7'-NH	7.40 (brs, 1H)	7.75 (brs, 1H)	7.98 (brs, 1H)	7.51 (brs, 1H)	7.96 (brs, 1H)	7.51 (brs, 1H, 7'-N-H)	7.63 (brs, 1H)	7.25 (brs, 1H)	7.60 (brs, 1H)
4-OMe and 6-OMe	4.02 (s, 6H)	3.98 (s, 6H)	4.00 (s, 6H)	3.99 (s, 6H)	4.05 (s, 6H)	4.03 (s, 6H)	4.03 (s, 6H)	4.00 (s, 6H)	4.00 (s, 6H)

Table 2. ¹³C NMR data of 1,3,5-triazine derivatives 7a–i.

Carbon	7a	7b	7c	7d	7e	7f	7g	7h	7i
2	169.88	163.36	166.70	169.70	166.70	166.70	166.70	166.70	166.70
4 and 6	169.34	169.23	170.50	170.30	170.55	170.50	170.90	170.50	170.50
1'	134.67	136.23	136.32	136.35	136.32	136.32	136.32	136.32	136.32
4'	131.43	135.44	135.63	136.14	135.11	136.11	136.11	136.11	136.11
2' and 6'	120.64	121.53	122.53	122.53	122.54	122.53	122.53	122.53	122.53
3' and 5'	121.63	125.82	122.82	122.86	122.82	122.82	122.82	122.82	122.82
8'	162.56	156.64	162.20	162.99	166.64	167.47	167.56	167.56	158.55
1''	133.77	–	138.22	121.46	133.99	141.87	130.86	122.42	–
4''	136.43	126.76	124.62	133.63	135.82	131.77	165.75	152.59	107.89
2'' and 6''	126.24	136.43 and –	128.32	161.04 and 128.22	133.89 and 128.36	96.62 and 129.06	130.00	130.93	121.30 and 111.23
3'' and 5''	127.35	128.36 and 133.65	146.96	116.19 and 124.83	130.69 and 128.00	140.56 and 128.43	115.33	114.35	112.33 and 156.20
7'', 8'' and 9''	–	–	–	–	–	–	–	–	113.78, 127.73 and 133.97
4-OMe and 6-OMe	54.17	54.17	54.17	54.17	54.17	54.17	54.17	54.17	54.17

Common protocol for the synthesis of target analogs (7a–i)

To an ice-cooled solution of compound **5** (1eq) in 5 ml of dimethylformamide, appropriate aromatic acids (**6a–i**; 1.5 eq), hydroxybenzotriazole (1.5 eq), EDC.HCl (2 eq) and few drops of triethylamine (TEA) were added and stirred at room temperature for 30–45 min. Finally, the resultants were dispensed into crushed ice. Then the formed precipitate was filtered, dried and recrystallized with ethanol to afford the products (**7a–i**) in yields mentioned.

4-chloro-N-(4-[(4,6-dimethoxy-1,3,5-triazin-2-yl)amino]phenyl)benzamide (7a)

Off-white solid, yield 72%; mp: 235–236°C; IR(KBr) ν_{max} : 3267, 3001, 2947, 1573, 1562, 1199, 821 cm^{-1} ; ¹H and ¹³C NMR: see Tables 1 & 2; ESI-MS *m/z*: 386.23 [M+H]⁺; 388.22 [M+H]⁺; Calcd. for C₁₈H₁₆ClN₅O₃

N-(4-[(4,6-dimethoxy-1,3,5-triazin-2-yl)amino]phenyl)thiophene-2-carboxamide (7b)

Light grey solid, yield: 71%; mp: 135–135°C; IR (KBr) ν_{\max} : 3275, 3001, 2947, 1697, 1577, 1562, 1365, 1199, 1111, 821 cm^{-1} ; ^1H and ^{13}C NMR: see Tables 1 & 2; ESI-MS m/z : 358.21 $[\text{M}+\text{H}]^+$; Calcd. for $\text{C}_{16}\text{H}_{15}\text{N}_6\text{O}_3\text{S}$

N-(4-[(4,6-dimethoxy-1,3,5-triazin-2-yl)amino]phenyl)-3,5-dinitrobenzamide (7c)

Yellowish green; yield: 71%; mp: 134–137°C; IR (KBr) ν_{\max} : 3448, 3448, 3082, 2993, 2947, 1662, 1543, 1477, 1365, 1234, 1103, 825 cm^{-1} ; ^1H and ^{13}C NMR: see Tables 1 & 2; ESI-MS m/z : 442.30 $[\text{M}+\text{H}]^+$; Calcd. for $\text{C}_{18}\text{H}_{15}\text{N}_7\text{O}_7$

N-(4-[(4,6-dimethoxy-1,3,5-triazin-2-yl)amino]phenyl)-2-fluorobenzamide (7d)

Off-white solid; yield 75%; mp: 117–119°C; IR(KBr) ν_{\max} : 3350, 3001, 2947, 1697, 1573, 1562, 1199, 821 cm^{-1} ; ^1H and ^{13}C NMR: see Tables 1 & 2; ESI-MS m/z : 370.24 $[\text{M}+\text{H}]^+$; Calcd. for $\text{C}_{18}\text{H}_{16}\text{FN}_5\text{O}_3$

2,4-dichloro-*N*-(4-[(4,6-dimethoxy-1,3,5-triazin-2-yl)amino]phenyl)benzamide (7e)

Off-white solid; yield: 73%; mp: 216–219°C; IR (KBr) ν_{\max} : 3360, 3140, 3001, 2912, 1678, 1573, 1531, 1199, 1111, 821 cm^{-1} ; ^1H and ^{13}C NMR: see Tables 1 & 2; ESI-MS m/z : 420.23 $[\text{M}+\text{H}]^+$; Calcd. for $\text{C}_{18}\text{H}_{15}\text{Cl}_2\text{N}_5\text{O}_3$

N-(4-[(4,6-dimethoxy-1,3,5-triazin-2-yl)amino]phenyl)-2-iodobenzamide (7f)

Reddish-brown solid; yield 72%; mp: 93–95°C; IR (KBr) ν_{\max} : 3487, 3298, 3001, 2947, 1639, 1573, 1562, 1365, 1199, 1111, 840, 821 cm^{-1} ; ^1H and ^{13}C NMR: see Tables 1 & 2; ESI-MS m/z : 478.21 $[\text{M}+\text{H}]^+$; Calcd. for $\text{C}_{18}\text{H}_{16}\text{IN}_5\text{O}_3$

N-(4-[(4,6-dimethoxy-1,3,5-triazin-2-yl)amino]phenyl)-4-fluorobenzamide (7g)

Off-white solid; yield: 72%; mp: 206–208°C; IR (KBr) ν_{\max} : 3271, 3147, 3063, 3001, 2951, 1697, 1585, 1512, 1369, 1199, 1157, 1111, 840 cm^{-1} ; ^1H and ^{13}C NMR: see Tables 1 & 2; ESI-MS m/z : 370.24 $[\text{M}+\text{H}]^+$; Calcd. for $\text{C}_{18}\text{H}_{16}\text{FN}_5\text{O}_3$

4-amino-*N*-(4-[(4,6-dimethoxy-1,3,5-triazin-2-yl)amino]phenyl)benzamide (7h)

Pale yellow solid; yield: 73%; mp: 147–150°C; IR (KBr) ν_{\max} : 3410, 3213, 3043, 2993, 1755, 1654, 1593, 1508, 1176, 1111, 837 cm^{-1} ; ^1H and ^{13}C NMR: see Tables 1 & 2; ESI-MS m/z : 367.33 $[\text{M}+\text{H}]^+$; Calcd. for $\text{C}_{18}\text{H}_{18}\text{N}_6\text{O}_3$

N-(4-[(4,6-dimethoxy-1,3,5-triazin-2-yl)amino]phenyl)-5-fluoro-1*H*-indole-2-carboxamide (7i)

Off-white solid; yield: 73%; mp: 160–162°C; IR (KBr) ν_{\max} : 3479, 3259, 3005, 2943, 1882, 1755, 1697, 1620, 1550, 1365, 1203, 1111, 821 cm^{-1} ; ^1H and ^{13}C NMR: see Tables 1 & 2; ESI-MS m/z : 409.31 $[\text{M}+\text{H}]^+$; Calcd. for $\text{C}_{20}\text{H}_{17}\text{FN}_6\text{O}_3$

Biology

Enzymes AChE (EC-3.1.1.7, from Electric Eel) and BChE (EC-3.1.1.8 from equine serum), substrates acetylthiocholine iodide (ATCh) and S-butylthiocholiniodide (BTCh) and reagents 2,2-azinobis(3-ethylbenzthiazoline-6-sulfonic acid) (ABTS) and 5,5'-dithiobis-2-nitrobenzoic acid were purchased from Sigma (USA), and phosphate-buffered saline (PBS) buffer and reference compounds Trolox and galantamine were procured from Merck (Darmstadt, Germany).

Biological assays

Anticholinesterase activity assay

The title compounds were tested for their inhibition activity against both AChE and BChE spectrophotometrically by the slightly modified Ellman method [17]. Phosphate buffer (pH 7.7, 200 mM) was freshly prepared and used for the experiments. First, 1 mM individual test samples in DMSO (end concentration 1%) were prepared and then diluted to the final concentration using 200 mM PBS (pH 7.7). The assay solution consisted of 145 μl PBS buffer, 80 μl of 5,5'-dithiobis-2-nitrobenzoic acid (18.5 mg of 5,5'-dithiobis-2-nitrobenzoic acid in 10 ml of PBS), 10 μl of AChE/BChE (4 mU/ml) and 10 μl test solution were taken into 96-well plate. Then, 15 μl of 1 mM corresponding substrate (ATCh/BTCh) was added and incubated for 5 min at 25°C. Absorbance variations

were detected at 415 nm by Bio-Rad ELISA microplate reader. The inhibition percentage was calculated from the following equation:

$$\text{Percent enzyme inhibition Activity} = 1 - \frac{A_t}{A_c} \times 100$$

where A_t and A_c are the absorbance of the test sample and absorbance of the control, respectively. Thus, IC_{50} values were determined from the concentration of inhibitor versus % of enzyme inhibition. Each sample was assessed in triplicate.

Kinetic studies on inhibition of AChE

To understand the mode of inhibition of highly potent compound **7c** on AChE, kinetic assessment was performed according to the reported Ellman's method [19]. Lineweaver–Burk plots were drawn by taking a static amount of AChE (0.4 U/mL) and varying concentrations of ATCh (0.1, 0.2, 0.3, 0.4 and 0.5 mM), with or without **7c** at varied amounts (2, 12 and 48 μ M). The experiments were carried out in 96-well plates, the same as the AChE inhibition activity, and the reaction was performed at a wavelength of 412 nm by ELISA Microplate Reader (Bio-Rad). The inhibition constants (K_{i1} and K_{i2}) of **7c** that were offered by slopes and intercepts of Lineweaver–Burk plots versus concentrations as the intercepts on the negative x-axis were determined.

Radical scavenging assay

The ABTS radical scavenging activity of titled compounds was measured using the partially modified method reported by Miller *et al.* [48]. Stock solution (8 mM) was prepared in water (10 ml) by dissolving ABTS (44 mg). ABTS radical cation ($ABTS^{\cdot+}$) was produced by the addition of 3 mM of potassium persulphate in equal volume to a stock solution for 14–20 h at room temperature in the dark. Fresh $ABTS^{\cdot+}$ work solution was prepared using methanol in a 1:29 ratio before the experiment. The test solution (10 μ l) along with 290 μ l of $ABTS^{\cdot+}$ solution in a 96-well microplate was incubated for 30 min. The absorbance was measured at 734 nm after initial mixing for 15 min by ELISA Microplate Reader (Bio-Rad). The parallel control assay was performed without an inhibitor. Trolox was used as a standard.

Docking studies

A preliminary molecular dynamics study on AChE (PDB: IC2O) was computed with GROMACS 4.5.5 software, with Gromacs96 54a7 force field. Simulations were carried out with a time step of 2 fs to get the free energy profiles. The trajectories were created up to 100 ns. The Linux cluster with 36 nodes (dual Xeon processor) was employed to perform simulations [3,49,50]. This simulated AChE structure was used in molecular docking studies of most active congener, **7c**, with the aid of the Autodock 4.2.3 program [51]. Applying the Lamarckian genetic algorithm method, molecular docking was done to find confirmations, binding sites and types of interactions of the molecule [52]. Insight-II/builder program (Discovery studio 3.5 software) was used to optimize the geometry of the target compound. To get suitable geometry of AChE active sites, hydrogen atoms were added, and water molecules and charges were removed. The blind docking was performed by setting a grid box with $126 \times 126 \times 126$ dimensions in the region of the binding site of AChE [53]. Docking parameters were set as 100 GA runs, 150 population size, 25,000 maximum number of energy evolutions and 27,000 maximum number of generations. In each docking simulation, 30 conformers were generated; the lowest free energy value conformer was used for further analysis [54].

Molecular dynamics study on AChE was done already, as the authors are working continuously on this enzyme for other molecules. The studied structure was selected for the present work and the enzyme was simulated for 100 ns.

Results & discussion

Chemistry

The cyanuric chloride (2,4,6 trichloro-1,3,5-triazine) was found to be the most important and an ideal starting material for the preparation of symmetrical and nonsymmetrical s-triazine analogs, as it is cheap and the best available chemical [18]. A series of triazineamide derivatives (**7a–i**) were synthesized using cyanuric chloride through a four-step process, as outlined in Figure 1. Initially, cyanuric chloride (**1**) was reacted with MeOH in the presence of

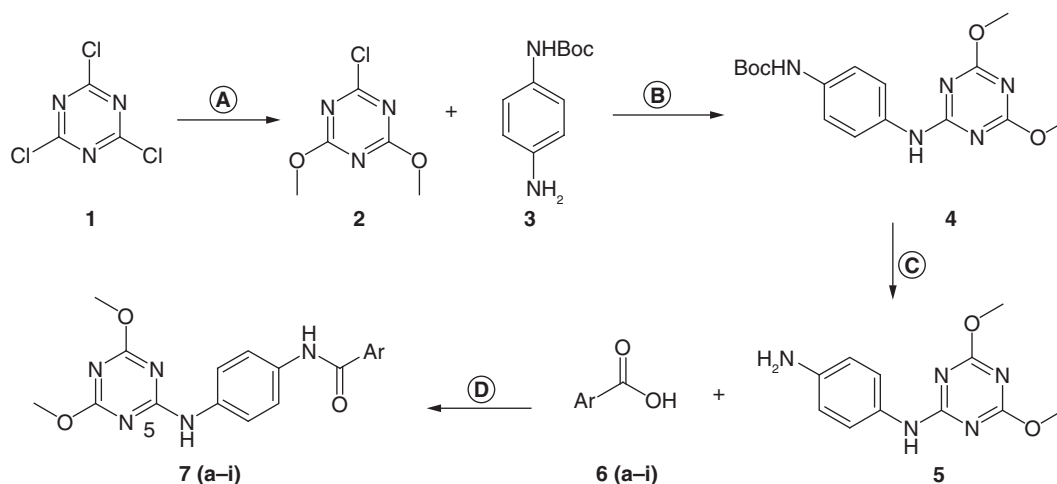


Figure 1. Synthesis of substituted N-(4-[(4,6-dimethoxy-1,3,5-triazin-2-yl)amino]phenyl)benzamide derivatives.
 Reagents and conditions: (A) NaHCO₃, MeOH, 0–50°C, 4 h; (B) acetone, Na₂CO₃, 0°C, 6 h; (C) 2N HCl, basify with NaOH; (D) EDC.HCl, hydroxybenzotriazole, triethylamine and dimethylformamide.

NaHCO₃ at 0°C to obtain compound **2** [25]. The obtained intermediate **2** was treated with 4-(Boc-amino)aniline to get N-Boc-triazine (**4**) [55]. Removal of the BOC in N-Boc-triazine intermediate (**4**) can be accomplished with strong acid HCl in dioxane at room temperature to yield N1-(4,6-dimethoxy-1,3,5-triazin-2-yl)benzene-1,4-diamine (**5**) [27]. Finally, compound **5** was treated with different substituted aromatic and heterocyclic acids (**6a–i**) in the presence of EDC.HCl, hydroxybenzotriazole and triethylamine in dimethylformamide to obtain the target compounds (**7a–i**) in good yields [28]. The stability of the compounds was thoroughly verified using physical and spectral methods. Target compounds were obtained as defined crystalline solids. During the determination of melting points, all solids melted sharply without decomposition. After 2 years, all the target compounds gave identical ¹H and ¹³C NMR without any additional signals. These factors confirmed the stability of the studied compounds. Finally, the structures of all the intermediates and target compounds were well characterized with the aid of spectroscopic (IR, ¹H NMR, ¹³C NMR and ESI–MS) data analysis. The IR absorptions revealed the presence of -HN, C=O of amide, aromatic C–H and aromatic C–F functionalities in the target molecules. In ¹H NMR, a set of A₂B₂ doublets in the range of δ 7.562–7.92 and δ 7.21–7.65 confirmed the para-phenylene diamine moiety in the molecule. Differently substituted aromatic moiety on amide group was elucidated with the proton signals in the aromatic range of δ 7.02–9.19. Two N–H groups (δ 7.72–9.15), (δ 7.25–7.98) and two methoxyl groups were resonated at δ 3.98–4.05 in the ¹H NMR spectra (Table 1). Accordingly, the ¹³C NMR spectra disclosed 18 signals for the carbon skeleton of target molecules in the appropriate regions. In particular, amide carbonyl (δ 156.64–167.56), three quarternary carbons of 1,3,5-triazene moiety (δ 163.36–169.88 and δ 169.23–170.90), four sets of carbons for the phenylene diamine scaffold (134.67–136.23; 131.43–136.14; 120.64–122.54 and 121.63–122.86) and two methoxyl carbons (δ 54.17) were seen in the ¹³C NMR spectra (Table 2).

Bioactivities

Inhibition of cholinesterase

To study the multipotent profiles of the titled triazineamide derivatives (**7a–i**), initially their inhibition potencies against AChE and BChE were assessed using the spectroscopic protocol adopted by Ellman *et al.* but with some modifications and galantamine used as a standard. IC₅₀ values offered the inhibition efficacy of titled analogs, as presented in Table 3. The tested triazineamides (**7a–i**) displayed varied inhibitory abilities on AChE, with IC₅₀ values in the range of 5.306 ± 0.002 to 9.234 ± 0.240 μM. Compound **7c**, with 3,5-dinitrobenzamido moiety, was found to have good AChE inhibition, with IC₅₀ value of 5.306 ± 0.002 μM. Overall, the monohalogenated benzamide analogs (**7a**, **7d**, **7f** and **7g**) exhibited significant anti-AChE activities. Compounds **7d** and **7f** with fluorine and iodine groups at *ortho* position of benzamide moiety executed similar inhibitory potency against AChE (IC₅₀: 7.221 ± 0.126 and 7.257 ± 0.092 μM). Introduction of one more chlorine atoms on the phenyl ring from **7a** (4-chloro, IC₅₀: 7.706 ± 0.012 μM) to **7e** (2,4-chloro, IC₅₀: 9.234 ± 0.240 μM) diminished the inhibitory

Table 3. Cholinesterase inhibition and 2,2-azinobis(3-ethylbenzthiazoline-6-sulfonic acid) radical scavenging capacities of triazineamide derivatives (7a–i), compound 5, galantamine and Trolox.

Compound	IC ₅₀ (μM) ± S.E.M. [†]		Selectivity ratio [§]	IC ₅₀ (μM) ± S.E.M. [†] 2,2-azinobis(3-ethylbenzthiazoline-6-sulfonic acid)
	Acetylcholinesterase [‡]	Butyrylcholinesterase [‡]		
7a	7.706 ± 0.012	>100	–	36.236 ± 1.64
7b	7.614 ± 0.021	96.834 ± 1.21	12.717	>50
7c	5.306 ± 0.002	>100	–	45.402 ± 0.865
7d	7.221 ± 0.126	73.479 ± 2.96	10.175	34.921 ± 1.82
7e	9.234 ± 0.240	89.837 ± 5.68	9.728	>50
7f	7.257 ± 0.092	85.370 ± 4.64	11.763	>50
7g	8.149 ± 0.667	>100	–	>50
7h	8.365 ± 0.373	>100	–	44.66 ± 1.77
7i	7.698 ± 0.542	>100	–	>50
5	8.784 ± 0.330	82.187 ± 1.97	9.356	46.343 ± 0.67
Galantamine	0.325 ± 0.026	22.021 ± 0.962	67.75	–
Trolox	–	–	–	24.93 ± 1.48

[†] Concentration required to produce 50% inhibition of enzyme activity. IC₅₀ values are given as the Standard error of mean (S.E.M) of three independent determinations.

[‡] AChE from Electric Eel and BChE from equine serum were used.

[§] Selectivity ratio = (IC₅₀ of BChE / IC₅₀ of AChE).

potency. Change in position of the fluorine atom, as in **7d** (2-fluoro) and **7g** (4-fluoro), lessened the activity against AChE. Interestingly, the congeners with heteroaromatic moieties such as thiazole (**7b**) with IC₅₀ value of 7.614 ± 0.021 μM and indole (**7i**) with IC₅₀ value of 7.698 ± 0.542 μM displayed similar activities. As far as BChE is concerned, few analogs, such as **5**, **7b**, **7d**, **7e** and **7f**, showed modest inhibitory activities with IC₅₀ in the range of 82.187 ± 1.97 to 96.834 ± 1.21 μM. Compound **7d** had better potency (IC₅₀: 73.479 ± 2.96 μM), comparatively. However, all the target compounds had less potency than galantamine (IC₅₀: 0.325 ± 0.026 μM for AChE and 22.021 ± 0.962 μM for BChE), a standard compound. From these observations, it is clear that the active analogs (**7b**, **7d**, **7e** and **7f**) have good inhibition selectivity against AChE over BChE, with selectivity index between 12.757 and 9.356, which could be advantageous to avoid cholinergic side effects and endowed with less harmfulness [56]. The severe side effects of tacrine, an AChE inhibitor have been ascribed to its poor selectivity only.

Kinetic study on AChE inhibition

To understand more about the inhibition approach of these 1,3,5-triazine benzamide derivatives, a kinetic study on AChE inhibition was carried out with the most potent congener, **7c**. In this study, the rate of the enzyme activity was determined using 0.1, 0.2, 0.3, 0.4 and 0.5 mM of the substrate ATCh (S) and 0.5, 1.5 and 2 μM of inhibitor **7c**. The double reciprocal plot was built with 1/v (v = initial velocity) versus 1/S (S = concentration of substrate). The resultant Lineweaver–Burk plot inferred the increasing slopes (decreased V_{max}) and intercepts (higher K_m) with increase in concentrations of **7c**, which is indicative of mixed-type inhibition [57]. From the secondary plots (i.e., slope vs concentration and intercept vs concentration), inhibitory constants (K_{i1} and K_{i2}) were calculated as 32.128 and 59.363 μM for compound **7c** and are shown in Figure 2. These results indicated that compound **7c** was capable of binding with both the catalytic active site (CAS) and the peripheral anionic site (PAS) of AChE [5,10].

Antioxidant activity

Lessening the oxidative stress might play a significant role in the development of anti-AD agents [58]. In view of this, in the present study the antioxidant capacities of **7a–i** and a standard compound, Trolox, were assayed using the ABTS radical scavenging method [5]. The radical scavenging capacities are expressed as IC₅₀ in Table 3. Target compounds **5**, **7a**, **7c**, **7d** and **7h** demonstrated effective ABTS radical scavenging activity with IC₅₀ values of 46.343 ± 0.67, 36.236 ± 1.64, 45.402 ± 0.865, 34.921 ± 1.82 and 44.66 ± 1.77 μM, respectively. However, all the target compounds exhibited less ABTS radical scavenging ability when compared with Trolox (IC₅₀: 24.93 ± 1.48 μM). Interestingly, all these analogs were active against AChE, which might be a beneficial feature of this new 1,3,5-triazine family in designing multifunctional agents against AD.

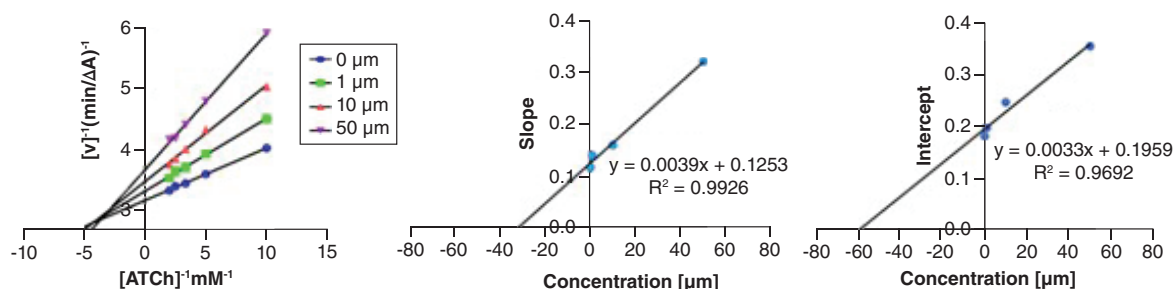


Figure 2. Kinetics of acetylcholinesterase inhibition for compound 7c. (Left) Lineweaver-Burk plot of 7c. (Right) Secondary plots: slope versus various concentrations of 7c and intercept versus various concentrations of 7c.

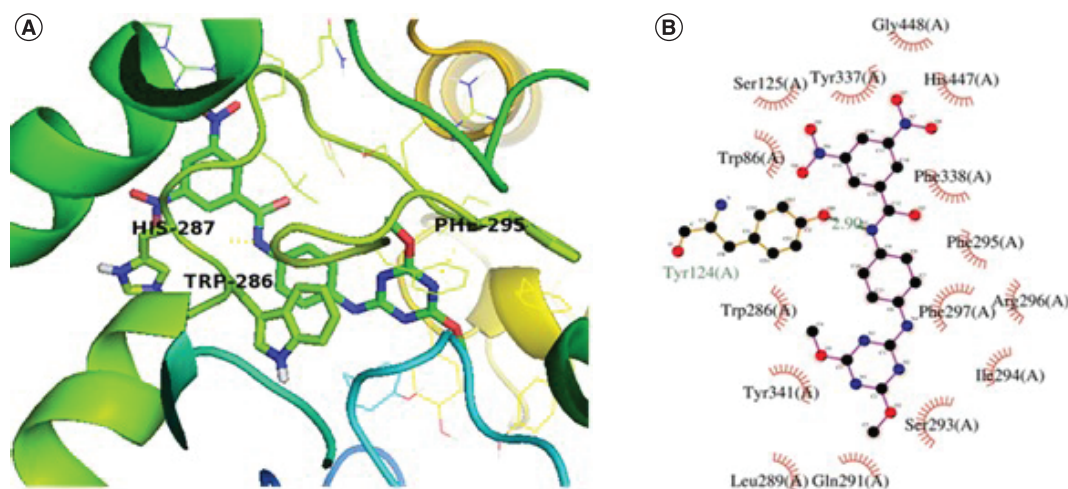


Figure 3. Docking pose of the most potent tested compound 7c at the binding site of AChE predicted by molecular modeling.

Molecular docking analysis

To support the potency of triazine amide derivatives against AChE activity (PDB: IC2O), a molecular docking analysis was carried out for 7c utilizing Autodock 4.2.3 software [59]. The crystallographic structure of AChE disclosed a 4.5 Å narrow gorge nearly 20 Å deep composed of two binding sites: a CAS at the bottom and a PAS at the entrance of the gorge. 30 conformations were generated during docking of 7c with AChE, among the 30 conformers, one with least binding free energy (-6.2 Kcal/mol) was selected as best docked pose for further analysis [60]. The docking pose and molecular interactions between residues in the AChE binding site and the functionalities of analog 7c are shown in Figure 3. From the docking pose, it is clear that the substituted triazine moiety of 7c was bound to the PAS of the enzyme and the dinitro benzamide fragment protruded into the CAS, as the phenylenediamine moiety spread in midgorge. Near the entry of the gorge, π - π stacking interactions were encountered between the phenyl ring of 7c and the indole ring of Trp286 residue in the PAS. Also, the -NH of the amide group had hydrogen bonding with hydroxyl moiety of Tyr124 in the CAS (2.99 Å). The dinitro benzamide fragment of 7c showed hydrophobic interactions with residues Trp86, Tyr337, Gly448 and Ser125 in the CAS. In addition, the phenylenediamine fragment was found to interact with Phe338, Phe295 and Phe297 via hydrophobic interactions, which assist in the recognition and orientation of the ligands in the active site. These observations designated that compound 7c exhibited a dual binding mode through simultaneous interaction with the CAS and PAS of AChE [61]. This type of dual binding agent could equally regulate the cholinergic and noncholinergic functions of AChE. Usually, compounds that bind to the CAS only might control the cholinergic activity of AChE i.e. ACh hydrolysis. Moreover, besides the hydrolysis capability of ACh, the PAS binding inhibitors were found to play a vital role in modulation of A β peptide aggregation, a key strategy that control initiation and progression of AD [61].

Conclusion

A series of triazineamide derivatives with an amidic linker between N1-(4,6-dimethoxy-1,3,5-triazin-2-yl)benzene-1,4-diamine and various aromatic acids was synthesized from the best available starting material, cyanuric chloride using nucleophilic substitution followed by condensation by simple and green methods. Most of the synthesized analogs displayed significant and selective AChE inhibition potency. This selectivity could be advantageous in avoiding peripheral cholinergic side effects caused by BChE inhibition and in providing lower toxicity [33]. Severe side effects of tacrine and its withdrawal as a drug have been ascribed to its poor selectivity only. N-(4-[(4,6-dimethoxy-1,3,5-triazin-2-yl)amino]phenyl)-3,5-dinitrobenzamide, **7c**, with an IC₅₀ value of $5.306 \pm 0.002 \mu\text{M}$, was the most potent AChE inhibitor. Kinetic study inferred a mixed pattern of inhibition for **7c** toward AChE. This property indicated that triazineamides may equally regulate the cholinergic and noncholinergic functions of AChE, which added benefit to controlling AD. Target compounds **7a**, **7c**, **7d** and **7h** also exhibited good ABTS radical scavenging activity. Molecular docking of **7c** with AChE disclosed that the compound was able to interact with both the CAS and the PAS of AChE, as indicated by kinetic study. A simple structure, an easy and eco-friendly method of synthesis, potent activity against AChE and ABTS, selectivity toward AChE over BChE and the dual inhibition ability of this family of triazineamide derivatives are the significant new findings of the present study, which led to wide scope for further development of these analogs as novel anti-AD drugs. Compound **7c** might be worthy of being chosen for further structure optimization studies to explore a new family of anti-AD agents. Structure–activity relationship studies, evaluations of noncholinergic activities, studies of multifunctional abilities and toxicity profiles followed by *in vivo* assay are the avenues for future work from these findings.

Summary points

- A series of triazineamide hybrids (**7a–i**) were designed and synthesized based on acetylcholinesterase (AChE) inhibition.
- Most of the synthesized analogs displayed significant and selective AChE inhibition potency.
- Simple starting materials and well-known protocols were used for their synthesis.
- One lead molecule, **7c**, showed potent inhibitory activity against AChE.
- Kinetic study inferred a mixed pattern of inhibition for the potent compound, **7c**, toward AChE.
- Target compounds **7a**, **7c**, **7d** and **7h** also exhibited good 2,2-azino-bis(3-ethylbenzthiazoline-6-sulfonic acid) radical scavenging activity.
- Molecular docking of **7c** with AChE disclosed that the compound was able to interact with both the catalytic active site and the peripheral anionic site of AChE, as indicated by kinetic study.
- Hybrid **7c** might be worthy of being chosen for further structure optimization studies to explore a new family of anti-AD agents.

Financial & competing interests disclosure

This work was supported through a research grant (EEQ/2017/000721) from SERB under EMEQ program, New Delhi, India. KY Rao (award no. 201920-NFST-AND-02583) would like to thank the Ministry of Tribal Welfare (Govt. of India) for providing financial support in the form of a national fellowship and scholarship for higher education of ST students (NFST). The authors have no other relevant affiliations or financial involvement with any organization or entity with a financial interest in or financial conflict with the subject matter or materials discussed in the manuscript apart from those disclosed.

No writing assistance was utilized in the production of this manuscript.

References

Papers of special note have been highlighted as: • of interest; •• of considerable interest

1. Anand P, Singh B. Synthesis and evaluation of novel carbamate-substituted flavanone derivatives as potent acetylcholinesterase inhibitors and anti-amnesic agents. *Med. Chem. Res.* 22(4), 1648–1659 (2013).
 2. Meng F-C, Mao F, Shan W-J, Quin F, Huang L, Li X-S. Design, synthesis, and evaluation of indanone derivatives as acetylcholinesterase inhibitors and metal-chelating agents. *Bioorg. Med. Chem. Lett.* 22(13), 4462–4466 (2012).
 3. Basha SJ, Subramanyam R, Damu AG *et al.* Deciphering the AChE-binding mechanism with multifunctional tricyclic coumarin anti-Alzheimer's agents using biophysical and bioinformatics approaches and evaluation of their modulating effect on amyloidogenic peptide assembly. *Int. J. Biol. Macromol.* 193(Pt B), 1409–1420 (2021).
- This article explained the need for the development of multitarget-directed ligands against Alzheimer's disease.

4. Shaik JB, Palaka BK, Gangaiah DA *et al.* Synthesis, biological evaluation and molecular docking of 8-imino-2-oxo-2H, 8H-pyrano [2,3-f] chromene analogues: new dual AChE inhibitors as potential drugs for the treatment of Alzheimer's disease. *Chem. Biol. Drug Design* 88(1), 43–53 (2016).
- **This article revealed the significance of dual acetylcholinesterase inhibitors against Alzheimer's disease.**
5. Shaik JB, Subramanyam R, Gangaiah DA *et al.* Synthesis and biological evaluation of flavone-8-acrylamide derivatives as potential multi-target-directed anti Alzheimer agents and investigation of binding mechanism with acetylcholinesterase. *Bioorg. Chem.* 88, 102960 (2019).
6. El-Gamal MI, Oh C-H. Synthesis *in vitro* antiproliferative activity, and *in silico*. *Eur. J. Med. Chem.* 84, 68–76 (2014).
7. Thirratmatrakul S, Yenjai C, Waiwut P *et al.* Synthesis, biological evaluation and molecular modeling study of novel tacrine-carbazole hybrids as potential multifunctional agents for the treatment of Alzheimer's disease. *Eur. J. Med. Chem.* 75, 21–30 (2014).
8. Rizzo S, Tarozzi A, Bartolini M *et al.* 2-Arylbenzofuran-based molecules as multipotent Alzheimer's disease modifying agents. *Eur. J. Med. Chem.* 58, 519–532 (2012).
9. Kozurkova M, Hamulakova S, Gazova Z, Paulikova H, Kristian P. Neuroactive multifunctional tacrine congeners with cholinesterase, anti-amyloid aggregation and neuroprotective properties. *Pharmaceuticals (Basel)* 4(2), 382–418 (2011).
10. Shaik JB, Kumar PB, Mohan P, Viswanath KK, Ramakrishna V, Gangaiah DA. Synthesis, pharmacological assessment, molecular modeling and *in silico*. *Eur. J. Med. Chem.* 107, 219–232 (2016).
- **This article disclosed the importance of multifunctional agents against Alzheimer's disease.**
11. Leopoldini M, Russo N, Toscano M. The molecular basis of working mechanism of natural polyphenolic antioxidants. *Food Chemistry* 125, 288–306 (2011).
- **This article explained various working mechanisms of antioxidants.**
12. He Y, Yao PF, Chen SB *et al.* Synthesis and evaluation of 7,8-dehydrorutaecarpine derivatives as potential multifunctional agents for the treatment of Alzheimer's disease. *Eur. J. Med. Chem.* 63, 299–312 (2013).
13. Bush AI, Tanzi RE. Therapeutics for Alzheimer's disease based on the metal hypothesis. *Neurotherapeutics* 5, 421–432 (2008).
14. Bush AI. Drug development based on the metals hypothesis of Alzheimer's disease. *J. Alzheimer Dis.* 15, 223–240 (2008).
15. Huang X, Moir RD, Tanzi RE, Bush AI, Rogers JT. Redox-active metals, oxidative stress, and Alzheimer's disease pathology. *Ann. NY Acad. Sci.* 1012, 153–163 (2004).
16. Gharat R, Prabhu A, Khambete MP. Potential of triazines in Alzheimer's disease: a versatile privileged scaffold. *Arch. Pharm.* 355, e2100388 (2022).
- **This review described in detail the structural properties and potency of various triazines against Alzheimer's disease.**
17. Ellman GL, Courtney KD, Andres V Jr, Feather-Stone RM. A new and rapid colorimetric determination of acetylcholinesterase activity. *Biochem. Pharmacol.* 7, 88–95 (1961).
18. Blotny G. Recent applications of 2,4,6-trichloro-1,3,5-triazine and its derivatives in organic synthesis. *Tetrahedron* 62, 9507–9522 (2006).
19. Basha SJ, Mohan P, Yeggoni DP, Babu ZR, Subramanyam R, Damu AG. New flavone-cyanoacetamide hybrids with a combination of cholinergic, antioxidant, modulation of β -amyloid aggregation, and neuroprotection properties as innovative multifunctional therapeutic candidates for Alzheimer's disease and unraveling their mechanism of action with acetylcholinesterase. *Mol. Pharm.* 15(6), 2206–2223 (2018).
- **This article explained multiple targets and hypotheses involved in the complex etiology of Alzheimer's disease.**
20. Goodford PJ. A computational procedure for determining energetically favorable binding sites on biologically important macromolecules. *J. Med. Chem.* 28(7), 849–857 (1985).
21. Avupati VR, Yejella RP, Parala VR *et al.* Synthesis, characterization and *in vitro*. *Bioorg. Med. Chem. Lett.* 23(21), 5968–5970 (2013).
- **This article talks about the medicinal importance of 1,3,5-triazines.**
22. Subramanyam R, Gollapudi A, Amooru DG *et al.* Novel binding studies of human serum albumin with *trans*. *J. Photochem. Photobiol. B* 95(2), 81–88 (2009).
23. Yeggoni DP, Rachamalla A, Subramanyam R. A comparative binding mechanism between human serum albumin and α -1-acid glycoprotein with corilagin: biophysical and computational approach. *RSC Adv.* 6, 40225–40237 (2016).
24. Malleda C, Ahalawat N, Gokara M, Subramanyam R. Molecular dynamics simulation studies of betulinic acid with human serum albumin. *J. Mol. Model.* 18, 2589–2597 (2012).
25. Xie S, Yan Z, Li Y, Song Q, Ma M. Intrinsically safe and shelf-stable diazo-transfer reagent for fast synthesis of diazo compounds. *J. Org. Chem.* 83(18), 10916–10921 (2018).
26. Clayden J, Rowbottom SJM, Hutchings MG, Ebenezer WJ. Formation of water-soluble sulfonated azacalix[4]arenes from cyanuric chloride. *Tetrahedron Lett.* 50(27), 3923–3925 (2009).
27. Karmakar A, Basha M, Venkatesh Babu GT *et al.* Tertiary-butoxycarbonyl (Boc) – a strategic group for N-protection/deprotection in the synthesis of various natural/unnatural N-unprotected amino acid cyanomethyl esters. *Tetrahedron Lett.* 59(48), 4267–4271 (2018).

28. Mane YD, Sarnikar YP, Surwase SM *et al.* Design, synthesis, and antimicrobial activity of novel 5-substituted indole-2-carboxamide derivatives. *Research on Chemical Intermediate* 43(2), 1253–1275 (2017).
29. Liston DR, Nielsen JA, Villalobos A *et al.* Pharmacology of selective acetylcholinesterase inhibitors: implications for use in Alzheimer's disease. *Eur. J. Pharmacol.* 486(1), 9–17 (2004).
30. Rampa A, Bisi A, Belluti F *et al.* Acetylcholinesterase inhibitors for potential use in Alzheimer's disease: molecular modeling, synthesis and kinetic evaluation of 11H-indeno-[1,2-b]-quinolin-10-ylamine derivatives. *Bioorg. Med. Chem.* 8(3), 497–506 (2000).
31. Nunomura A, Castellani RJ, Zhu X, Moreira PI, Perry G, Smith MA. Involvement of oxidative stress in Alzheimer disease. *J. Neuropathol. Exp. Neurol.* 65(7), 631–641 (2006).
32. Jones G, Willett P, Glen RC, Leach AR, Taylor R. Development and validation of a genetic algorithm for flexible docking. *J. Mol. Biol.* 267(3), 727–748 (1997).
33. Sunduru N, Gupta L, Chaturvedi V, Dwivedi R, Sinha S, Prem Chauhan MS. Discovery of new 1,3,5-triazine scaffolds with potent activity against-feruloylmaslinic acid. *J. Photochem. Photobiol. B* 95(2), 81–88 (2009).
34. Zhou C, Min J, Liu Z *et al.* Synthesis and biological evaluation of novel 1,3,5-triazine derivatives as antimicrobial agents. *Bioorg. Med. Chem. Lett.* 18, 1308–1311 (2008).
35. Ng H-L, Ma X, Chew E-H, Chui W-K. Design, synthesis, and biological evaluation of coupled bioactive scaffolds as potential anticancer agents for dual targeting of dihydrofolate reductase and thioredoxin reductase. *J. Med. Chem.* 60, 1734–1745 (2017).
36. Nishimura N, Kato A, Meeba I. Synthesis of pyrrolo[2,1-f][1,2,4]triazine C-nucleosides. Isosteres of sangivamycin, tubercidin, and roycamycin. *Carbohydrate Res.* 331, 77–82 (2001).
37. Mibu N, Kazumi Y, Aki H *et al.* Synthesis and antiviral evaluation of some C3-symmetrical trialkoxy substituted 1,3,5-triazines and their molecular geometry. *Chem. Pharm. Bull.* 63(11), 935–944 (2015).
38. Bahar AA, Liu Z, Garafalo M, Kallenbach N, Ren D. Controlling persister and biofilm cells of Gram-negative bacteria with a new 1,3,5-triazine derivative. *Pharmaceuticals (Basel)* 8(4), 696–710 (2015).
39. Sarmah KN, Sarmah NK, Kurmi KB, Patel TV. Synthesis and studies of antifungal activity of 2,4,6-trisubstituted 1,3,5-triazines. *Adv. Appl. Sci. Res.* 3(3), 1459–1462 (2012).
40. Zacharie B, Abbott SD, Bienvenu J-F *et al.* 2,4,6-trisubstituted triazines as protein a mimetics for the treatment of autoimmune diseases. *J. Med. Chem.* 53(3), 1138–1145 (2010).
41. Klenke B, Stewart M, Barrett MP, Brun R, Gilbert IH. Synthesis and biological evaluation of s-triazine substituted polyamines as potential new anti-trypanosomal drugs. *J. Med. Chem.* 44(21), 3440–3452 (2001).
42. Lolak N, Tuneğ M, Doğan A, Boğa M, Akocak S. Synthesis and biological evaluation of 1,3,5-triazine-substituted ureido benzenesulfonamides as antioxidant, acetylcholinesterase and butyrylcholinesterase inhibitor. *Bioorg. Med. Chem. Rep.* 3(2), 22 (2020).
43. Lolak N, Boga M, Tuneg M, Karakoc G, Akocak S, Supuran CT. Sulphonamides incorporating 1,3,5-triazine structural motifs show antioxidant, acetylcholinesterase, butyrylcholinesterase, and tyrosinase inhibitory pro. *J. Enzyme Inhib. Med. Chem.* 35(1), 424 (2020).
44. Iraj A, Firuzi O, Khoshneviszadeh M, Nadri H, Edraki N, Miri R. Synthesis and structure-activity relationship study of multi-target triazine derivatives as innovative candidates for treatment of Alzheimer's disease. *Bioorg. Chem.* 77, 223 (2018).
45. Yazdani M, Edraki N, Badri R, Khoshneviszadeh M, Iraj A, Firuzi O. Multi-target inhibitors against Alzheimer disease derived from 3-hydrazinyl 1,2,4-triazine scaffold containing pendant phenoxy methyl-1,2,3-triazole: Design, synthesis and biological evaluation. *Bioorg. Chem.* 84, 363 (2019).
46. Gonzalez P, Pota K, Turan LS, Da Costa VCP, Akkaraju G, Green KN. Synthesis, Characterization, and Activity of a Triazine Bridged Antioxidant Small Molecule. *ACS Chem. Neurosci.* 8(11), 2414 (2017).
47. Maqbool M, Manral A, Jameel E *et al.* Development of cyanopyridine-triazine hybrids as lead multitarget anti-Alzheimer agents. *Bioorg. Med. Chem.* 24(12), 2777 (2016).
48. Thirratmatrakul S, Yenjai C, Waiwut P *et al.* Synthesis, biological evaluation and molecular modeling study of novel tacrine-carbazole hybrids as potential multifunctional agents for the treatment of Alzheimer's disease. *Eur. J. Med. Chem.* 75, 21–30 (2014).
- **This article contains the protocols of bioassays and molecular modeling related to the targets of Alzheimer's disease.**
49. Pronk S, Pall S, Schulz R *et al.* GROMACS 4.5: a high-throughput and highly parallel open source molecular simulation toolkit. *Bioinformatics (Oxford, England)* 29, 845–854 (2013).
50. Schuttelkopf AW, van Aalten DM. PRODRG: a tool for high-throughput crystallography of protein-ligand complexes, acta crystallographica. *Acta Crystallogr. D Biol. Crystallogr.* 60, 1355–1363 (2004).
51. Subramanyam R, Goud M, Amooru DG *et al.* Novel binding studies of human serum albumin with trans-feruloylmaslinic acid. *J. Photochem. Photobiol. B* 95(2), 81–88 (2009).
52. Pushparaju Yeggoni D, Rachamallu A, Subramanyam R. A comparative binding mechanism between human serum albumin and α -1-acid glycoprotein with corilagin: biophysical and computational approach. *RSC Adv.* 6, 40225–40237 (2016).
53. Goodford PJ. A computational procedure for determining energetically favorable binding sites on biologically important macromolecules. *J. Med. Chem.* 28(7), 849–857 (1985).

54. Malleda C, Ahalawat N, Gokara M, Subramanyam R. Molecular dynamics simulation studies of betulinic acid with human serum albumin. *J. Mol. Model.* 18, 2589–2597 (2012).
55. Clayden J, Rowbottom SJM, Hutchings MG, Ebenezer WJ. Formation of water-soluble sulfonated azacalix[4]arenes from cyanuric chloride. *Tetrahedron Lett.* 50(27), 3923–3925 (2009).
56. Liston DR, Nielsen JA, Villalobos A *et al.* Pharmacology of selective acetylcholinesterase inhibitors: implications for use in Alzheimer's disease. *Eur. J. Pharmacol.* 486(1), 9–17 (2004).
57. Rampa A, Bisi A, Belluti F *et al.* Acetylcholinesterase inhibitors for potential use in Alzheimer's disease: molecular modeling, synthesis and kinetic evaluation of 11H-indeno-[1,2-b]-quinolin-10-ylamine derivatives. *Bioorg. Med. Chem.* 8(3), 497–506 (2000).
58. Nunomura A, Castellani RJ, Zhu X, Moreira PI, Perry G, Smith MA. Involvement of oxidative stress in Alzheimer disease. *J. Neuropathol. Exp. Neurol.* 65(7), 631–641 (2006).
59. Jones G, Willett P, Glen RC, Leach AR, Taylor R. Development and validation of a genetic algorithm for flexible docking. *J. Mol. Biol.* 267(3), 727–748 (1997).
60. Li R-S, Wang X-B, Hu X-J, Kong L-Y. Design, synthesis and evaluation of flavonoid derivatives as potential multifunctional acetylcholinesterase inhibitors against Alzheimer's disease. *Bioorg. Med. Chem. Lett.* 23(9), 2636–2641 (2013).
61. Bolognesi ML, Andrisano V, Bartolini M, Banzi R, Melchiorre C. Propidiumbased polyamine ligands as potent inhibitors of acetylcholinesterase and acetylcholinesterase-induced amyloid- β aggregation. *J. Med. Chem.* 48(1), 24–27 (2005).